

Impact of vegetation fires on composition and circulation of the atmosphere (EFEU)

Sabine Wurzler*, Martin Simmel*, and the EFEU-Team**

simmel@tropos.de

*:Leibniz-Institut für Troposphärenforschung, Permoserstr. 15, D-04318 Leipzig **: Institut für Meteorologie der Universität Leipzig; Max-Planck-Institut für Meteorologie, Hamburg; Max-Planck-Institut für Chemie, Biogeochemie, Mainz, and Leibniz-Institut für Troposphärenforschung, Leipzig.

<http://projects.tropos.de:8088/afo2000g3/>

Scientific objectives

Vegetation fires are a significant source for atmospheric trace gases and aerosol particles (AP) on both local and global scale. Vast fires regularly occur in the tropics (Africa, South America, and South East Asia) as well as in the mid latitudes and boreal regions (the Mediterranean region, USA, Canada, Scandinavia, and Russia). Fire emissions and their reaction products are transported by convection into the free troposphere and the lower stratosphere and are distributed from the local scale to the mesoscale and even to the global scale.



Figure 1: Clouds forming in the plume of a vegetation fire (photo: Wurzler).

Particles and gases from vegetation fires and their secondary products change the chemical composition of the atmosphere. Their influence on cloud microphysics (Fig. 1) may lead to warm precipitation suppression and a vertical shift in the release of latent heat. This has significant effects on the atmospheric energy and radiation budget (direct and indirect effects) and potentially on the global circulation. Fig. 2 summarizes the various processes connected with biomass burning and their interactions on different scales.

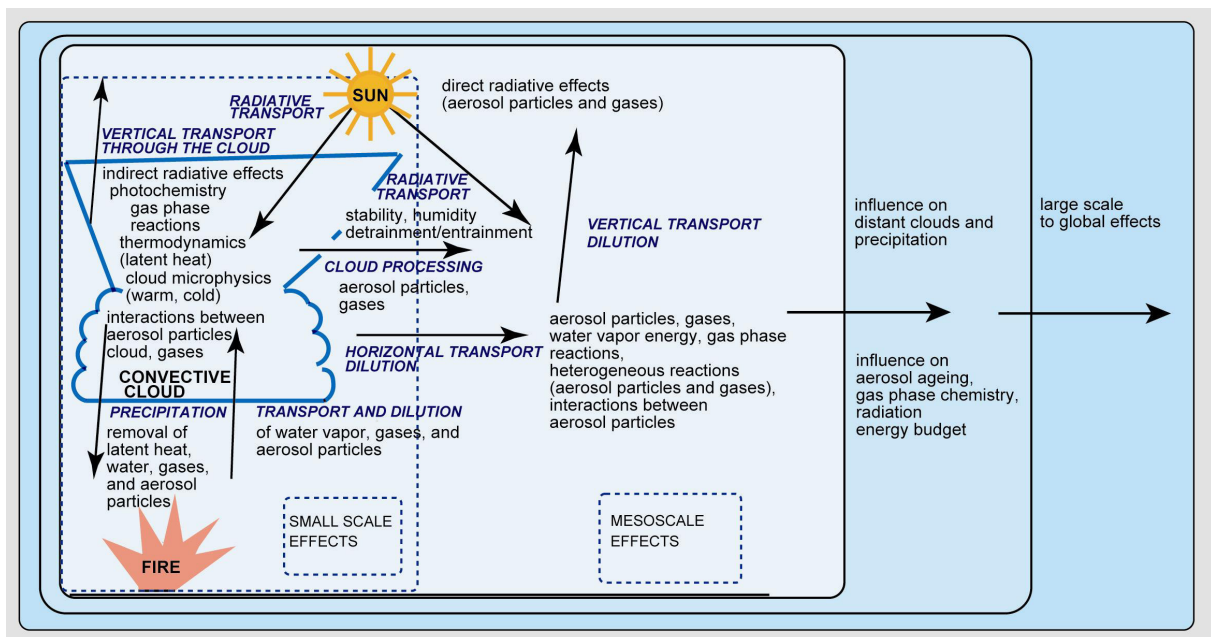


Figure 2: Schematic summary of the effects of vegetation fires on atmospheric physics and chemistry from the small to the large scale

The joint research project EFEU addresses the following questions:

1. What is the contribution of vegetation fires to the local trace gas and particle budgets of the troposphere and the lower stratosphere?
2. To which extent do aerosols emitted from vegetation fires affect the radiation budget of the atmosphere (direct effect)?
3. How does vertical transport of fire emissions into the upper troposphere influence cloud formation and chemical and microphysical processes in clouds?
4. How relevant is the change of microphysical properties caused by aerosols from biomass burning for the regional radiation (indirect effect) and energy budgets of the atmosphere and the small-scale atmospheric circulation?

Methods

These questions are addressed with a combined experimental and numerical approach drawing from the expertise of eight different research groups. The experimental part is designed to enhance the database on biomass burning emissions with a particular focus on the suite of input parameters required by the numerical models employed in the EFEU project. Controlled burn experiments were performed with various types of typical biomass burning fuel ranging from central European to tropical fuel types. During these experiments physical, optical and chemical particulate parameters as well as a limited number of gas phase species are characterized. Among the measurement parameters are:

- optical absorption and scattering coefficients of aerosol particles
- total particle concentration and number size distribution (12 nm to 10,000 nm in diameter)
- morphological and chemical characterization of aerosol particles by single particle analysis
- bulk and size resolved chemical and mass characterization of particulate matter
- hygroscopic growth factors of the particles and CCN/CN ratios
- trace gas abundances of NO, CO and CO₂

Two series of laboratory experiments took place in May/June 2002 and June 2003 at the laboratory oven of the MPI Mainz (see Fig. 3). While in the first campaign, African (e.g., acacia, musasa, mupangara) and Mediterranean (e.g., aleppo pine, kermes oak) vegetation has been investigated, the second campaign focused on biomass from boreal regions (oak, spruce, pine; partly with dry or green material). A third campaign was carried out in September 2003 in order to establish reproducibility of the measurements and to investigate emissions from Indonesian and German peat fires.



Figure 3: Laboratory oven facility at MPI Mainz (reproduced with the permission of J. Lelieveld).

A hierarchically structured suite of originally independent numerical models is employed to investigate the complex impact of biomass burning emissions on the atmosphere. The various model components complement each other addressing different aspects of this topic on a range of spatial and temporal scales. Combined with the input data from the laboratory experiments this integrated approach allows a more complete view on physical, chemical and dynamical aspects of biomass burning plumes. The model hierarchy facilitates seamless transition from microscale to regional scale models and spans the temporal scale from a few minutes to months and years. Among other aspects the modelling efforts address:

- impact of biomass burning aerosol on cloud microphysics and precipitation using detailed and parameterized model approaches including the ice phase
- evolution of individual biomass burning plumes, considering dynamical evolution and troposphere-stratosphere exchange of emissions as well as chemical processes in young plumes
- effect of radiative transport on chemistry and dynamics of the atmosphere and determination of the role of biomass burning on the regional climate
- effect of biomass burning on the atmospheric budgets of trace constituents, water, and energy on the regional scale

Selected results

Optical properties of the biomass burning aerosol: Modelling the impact of vegetation fires on radiative transport requires accurate knowledge of the optical properties of biomass burning aerosol. Optical properties of particles are well described by Mie theory and mainly depend on particle size, shape, and index of refraction m . However, for biomass burning aerosol especially m is not well known. The EFEU data set provides the unique opportunity to investigate m for various fuel types and burning conditions. As an example Fig. 4 shows 2-minute averages of the measured SSA (single scattering albedo = ratio of scattering and extinction coefficient) at a wavelength of 550 nm of about 9-minutes old biomass burning aerosol from an oak (dry) fire; the corresponding burning conditions are also shown as dCO/dCO_2 trace (crosses), where dCO and dCO_2 represent CO and CO_2 concentrations above background levels. There was an obvious positive correlation between SSA and dCO/dCO_2 . In the smouldering phase at the beginning of the experiment ($dCO/dCO_2 > 8\%$) SSA was very high with values around 0.95. With the start of the flaming combustion ($dCO/dCO_2 < 8\%$) at 11:33 SSA showed a sharp decrease down to approximately 0.7 followed by a relatively steady increase to just above 0.9 accompanied by an increase in dCO/dCO_2 .

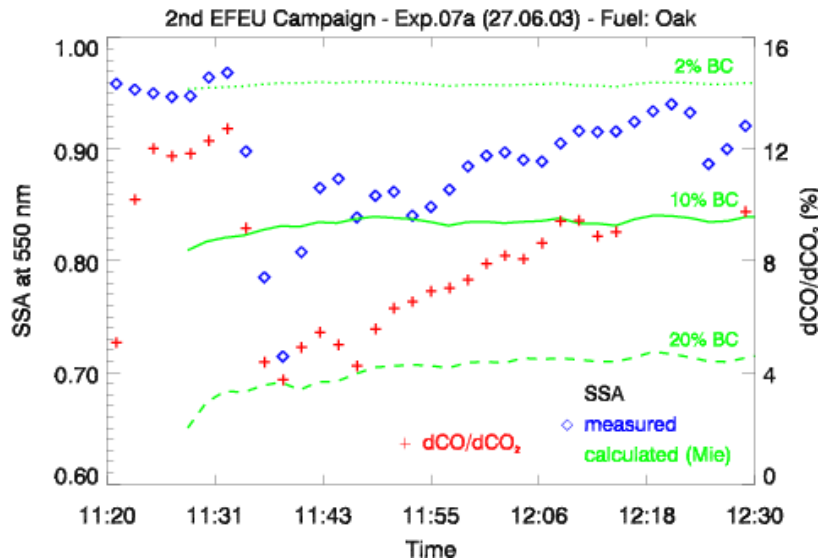


Figure 4: Comparison between measured and modelled single scattering albedo (SSA) for a 1-hour fire with dry oak as fuel.

For comparison, Fig. 4 also shows Mie calculations of the SSA for three different black carbon (BC) mass fractions based on the measured number size distributions under the assumption of spherical particle shape which is justified by SEM pictures. Due to the significantly lower volatility of black carbon (BC) compared to organic carbon (OC) we performed the Mie calculations for coated spheres with a BC core ($m_{BC} = 1.75-0.44i$) and an OC shell ($m_{OC} = 1.53-0.0i$). Fig. 4 shows that the modelled SSA is fairly constant for each BC mass fraction. Hence, changes in size distribution alone cannot explain the observed variations in SSA which indicates a significant role of particle chemistry and hence m . We found that BC mass fractions of 2 and 20% represent the observed extreme SSA values of about 0.95 and 0.7, respectively, reasonably well. This is consistent with the expected higher BC content for more flaming fires (lower dCO/dCO_2 values) which produce higher combustion temperatures and consequently more soot. Hence, our results suggest that young biomass burning aerosol may be modelled as BC spheres coated with a variable amount of OC depending on the burning conditions. Similar Mie calculations will be performed for all of the wood types investigated in the EFEU laboratory campaign and then hopefully condensed into a single parameterization at least for certain categories of wood (e.g. northern boreal, tropical, peat, etc.).

Drop nucleation ability of the aerosol particles: As a step for the understanding of the influence of biomass burning aerosol on cloud formation, potential cloud condensation nuclei (CCN) were identified by determining the CCN/CN ratio in the laboratory experiments. This was done for different dry particle sizes (50, 100, 150, 250, and 325 nm) at different supersaturations from 0.24 to 1.64 %. The experimental results are compared to critical supersaturations calculated from extended Köhler theory which is also used in the detailed microphysical models applied in the project. Fig. 5 shows the critical supersaturation for varying ϵ (soluble fraction, here ammonium sulphate) and AP sizes (lines with different colors). CCN/CN ratios of 25 (circles), 50 (squares), 75 (diamonds), and 100 % (triangles) are deduced from the measurements and compared to the theoretical values. The black

square on the red line means, e.g., that 50 % of the 100 nm AP are activated at 0.46 % supersaturation which corresponds to a theoretical value of $\epsilon = 0.08$. One can see that the soluble fraction generally is small ($\epsilon < 10\%$ for about 50 % of the particles) as it is expected for biomass burning AP and that ϵ is slightly higher for smaller AP sizes (50 nm vs. 150 nm). Despite their small ϵ , larger particles (150, 200 nm) are activated at relatively low supersaturations that easily could be reached in clouds. Obviously, the critical supersaturations are very sensitive to $\epsilon < 20\%$ especially for smaller sizes (50, 100 nm).

Therefore, small changes in epsilon could highly influence the number of drops in clouds affected by biomass burning. The CCN/CN ratios are quite similar for the different wood types (spruce, pine, oak, and musasa) considered in the EFEU experiments.

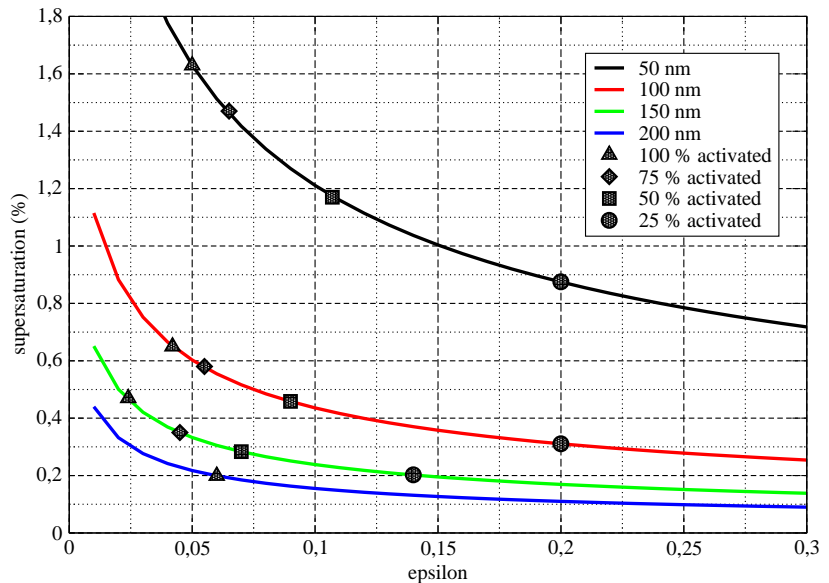
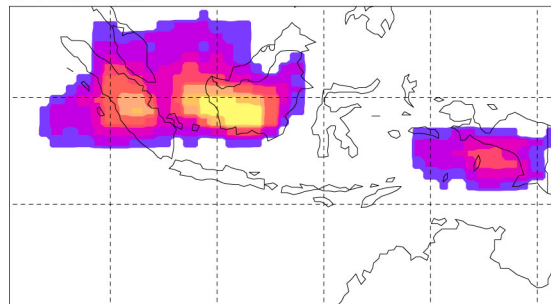


Figure 5: Critical supersaturations (lines) and CCN/CN ratios (symbols) for different AP sizes and solubilities.

Modelling results from the regional model REMO: The spatial distribution of smoke haze in Indonesia in 1997 can be derived from the TOMS Aerosol Index (AI) data, shown as monthly mean in the upper part of Fig. 6. During the smoke haze period maximum intensity in TOMS AI data is visible in the provinces of South Sumatra, Jambi, Central and West Kalimantan, and on Irian Jaya, where the main

TOMS AI



REMO: TPM [mg(C)/m²]

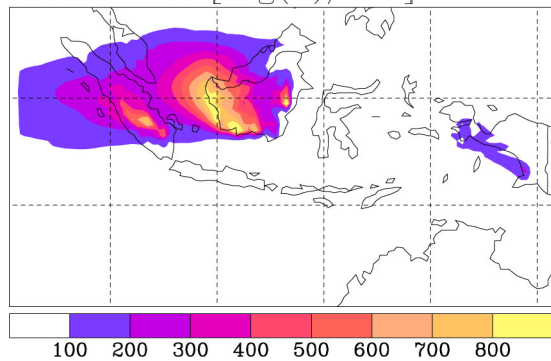


Figure 6: Comparison of TOMS AI data over Indonesia with REMO TPM results for September 1997.

peat fire emission areas are located. Large scale transport from these source regions to northern and western directions reaching into the Indian Ocean occurred especially during September 1997, when the fire emissions were highest and rainfall and associated wet deposition was lowest.

The lower part of Fig. 6 presents the monthly mean atmospheric column burden in mg(C)/m² of total particulate matter (TPM) as determined by the regional model REMO. It should be emphasised at this point that Fig. 6 displays only a qualitative comparison of TOMS AI with REMO calculated TPM in order to evaluate the simulated temporal and spatial distribution of smoke haze. The principle ability of the REMO model to reproduce the spatial and temporal distribution of TPM is clearly visible from Fig. 6. A north-west transport of smoke haze dominated in September 1997. Compared to TOMS AI the intensity of the smoke haze originating from Irian Jaya is relatively low. These differences in modelled and observed smoke haze distribution can result from the fact that TOMS AI cannot detect absorbing aerosols at altitudes below about 1 km because of the underlying Rayleigh scattering.